Pergamon

Adv. Space Res. Vol. 20, No. 3, pp. 369–372, 1997
Published by Elsevier Science Ltd on behalf of COSPAR
Printed in Great Britain
0273-1177/97 $17.00 + 0.00

PII: S0273-1177(97)00693-5

SPATIAL DISTRIBUTIONS OF THE INNER RADIATION BELT ELECTRONS: A COMPARISON BETWEEN OBSERVATIONS AND RADIAL DIFFUSION THEORY PREDICTIONS

D. M. Boscher,*,** S. F. Fung* and L. C. Tan*,***

* *Space Physics Data Facility, NASA Goddard Space Flight Center, Greenbelt, MD 20771, U.S.A.*
** *On leave from CERT/ONERA, Toulouse, France*
*** *Also at the Hughes STX Corporation, Greenbelt, MD 20770, U.S.A.*

ABSTRACT

It is well known that the quiet-time electron radiation belts exhibit a two-zone radial structure. Although the inner radiation belt does show dynamic variations during geomagnetically active periods, the stably trapped electrons found in this region are thought to be populated primarily by diffusive transport processes. Recent analyses of the long-term (1984-1987) energetic electron (0.19-3.2 MeV) observations taken at 350-850 km altitude by the OHZORA satellite indicate that the trapped electrons also show local-time variations in pitch angle distributions. We here report the observed L-shell distributions of the energetic electrons and show that they are in good agreement with the azimuthally averaged predictions of the radial diffusion theory (the Salammbo model) for inner zone electron fluxes. We also compare the OHZORA observations with earlier observations as compiled in the NASA empirical radiation belt models.
Published by Elsevier Science Ltd on behalf of COSPAR

INTRODUCTION

The study of trapped radiation is important because the radiation belts are integral parts of the Earth's magnetosphere. The structure and dynamics of the radiation belts are intimately connected to and affected by many geophysical phenomena, such as geomagnetic storms and substorms. Over the years, however, analyses of space observations and theoretical investigations have yielded only semi-quantitative understanding of the trapped particle radiation in terms of the effects of various magnetospheric processes on the otherwise adiabatic motions of the trapped particles (Spjeldvik and Rothwell, 1985; Schulz and Lanzerotti, 1974; Roederer, 1970). We have yet to fully understand the occurrences (spatial and temporal) of the trapped particle radiation and their associated energy and pitch angle distributions.

Despite the apparent agreement between theory and observations regarding the existence of the quiet-time electron slot region (Lyons *et al.*, 1972; Lyons and Thorne, 1973), the detailed structure of the slot region in local time and in latitude (Fung *et al.*, 1996), and how it depends on the presence of plasma waves are not well established. Interaction with magnetospheric plasma waves is an important transport and loss mechanisms for the energetic particles trapped in the earth's magnetic field. Radial diffusion transports energetic particles injected into the high L-shells (near L=6) during a geomagnetic storm into lower L-shells (down to L<2). Pitch-angle scattering causes precipitation of the charged particles into the ionosphere.

In order to properly model the trapped radiation environment, we have to account for all the loss mechanisms that will operate on a given species of energetic particles. Since Coulomb interactions are relatively straightforward when the corresponding interaction cross sections are provided, more uncertainties are involved with the wave-particle interaction and diffusive processes. This paper examine the spatial distribution of trapped electrons at low altitudes as resulting from radial-, pitch angle-, and energy- diffusions, so that their effects can be quantitatively tested.

MODEL DESCRIPTION AND INITIALIZATION

The three dimensional Salammbo model based on the classical Fokker-Planck diffusion equation has been used to calculate the electron transport in the region of magnetosphere with $1.02 < L < 7$, where L is the generalized McIlwain parameter (Beutier and Boscher, 1995). The full three-dimensional model is necessary to properly treat pitch angle diffusion of electrons, either given by Coulomb collisions or by wave-particle interactions. In the model, the transport equation in the three phase space coordinates (the relativistic magnetic moment M, the second invariant J and the shell magnetic flux) is solved numerically. The explicit finite differencing scheme with logarithmic steps in M, J, and L for solving the transport equation has been described in detail in Beutier and Boscher (1995). The Salammbo model fully treats radial and pitch angle diffusion as well as frictional interactions with free (plasmaspheric) and bounded (exospheric) electrons.

The friction terms and pitch angle transport coefficients have been calculated using an eccentric tilted dipole field consistent with the International Geomagnetic Reference Field (IGRF) for 1986 to provide the correct epoch for comparing with the OHZORA observations. The lower atmospheric boundary model is given by an exospheric model derived from the Mass Spectrometer and Incoherent Scatter (MSIS)-86 model (available from the NASA National Space Science Data Center) which is also used for the Coulomb collision calculations. The upper boundary of our model is located at $L = 7$ with the equilibrium trapped electron fluxes prescribed by the NASA AE8-MIN model (Vette, 1992). The radial diffusion coefficients (appropriate for the magnetic and electric perturbations) used were a factor of 10 less than those given in Schulz (1991) in order to obtain good flux agreement in the inner belt region; *i.e.*, $D_{LLM} = 8.0\ 10^{-15}\ f(y)\ L^{10}$ and $D_{LLE} = 1.2\ 10^{-16}\ g(y)\ h(M,y,L)\ L^{6}$, where the functions f(y), g(y) and h(M,y,L) are as given in Schulz (1991).

The pitch angle diffusion coefficients were calculated as in Lyons *et al.* (1972), but with wave characteristics as deduced from Thorne *et al.* (1973), *i.e.*, an average wave amplitude of 35 nT, a mean frequency of 190 Hz, a bandwidth of 400 Hz and a lower cutoff frequency of 140 Hz. In order to obtain a dayside slot region consistent with observations (Fung *et al.*, 1996), the wave distribution in L-shell was taken to have a trapezoidal form shown in Figure 1 where the maximum value corresponds to the observed average amplitude.

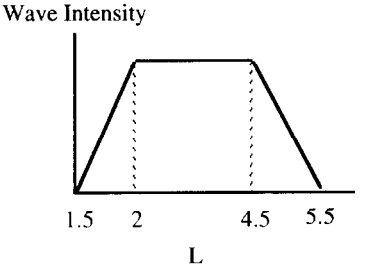

Figure 1. Model Plasmaspheric Hiss L-Shell Distribution

The electron distribution functions were initially assumed to be zero everywhere in the computation box (L between 1.02 and 7). Then the code runs until a steady state is obtained. The resultant distribution functions are then converted into uni- or omnidirectional fluxes. For comparisons with observations and the AE8 model, integral omnidirectional fluxes in units of $cm^{-2}s^{-1}$ were calculated.

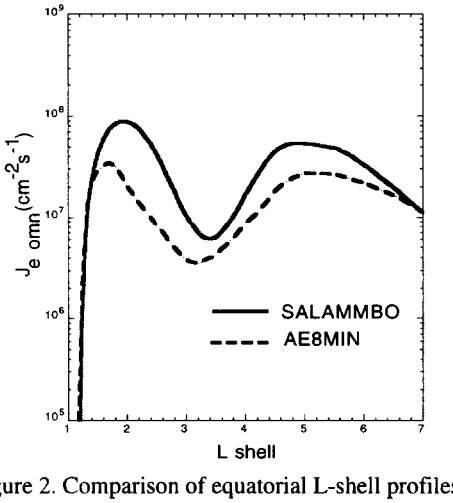

Figure 2. Comparison of equatorial L-shell profiles of omnidirectional trapped electron fluxes (> 0.2 MeV) predicted by the SALAMMBO and AE-8MIN models.

MODEL RESULTS

The results of our model calculations are shown in Figures 2, 3, and 4, and are compared to fluxes from the NASA AE8-MIN model and to the OHZORA observations (Nagata *et al.*, 1985; Kohno *et al.*, 1990; Fung *et al.*, 1996). Figure 2 shows a comparison of the equatorial L-shell profiles of integral omnidirectional fluxes of trapped electrons obtained from the Salammbo and the NASA AE8-MIN models. Since the AE8-MIN fluxes were used as boundary conditions at $L = 7$, the fluxes from the two models are identical. At lower L values, there is good qualitative agreement between the two models and the discrepancies never exceed a factor of 5. It should be noted that the AE8

model corresponds only to an average of fluxes which are drastically varying in the outer belt (L > 3) (Baker et al., 1994), which in turn will influence the dynamic structure of the radiation belts at lower L values.

Figure 3 presents model calculations of the global distributions of trapped electron at the altitudes of 400 km (left panel) and 800 km (right panel). The IGRF-86 model has been used to project the results obtained with the tilted dipole field to various locations at a given altitude. We can note here that the distributions shown are qualitatively similar to the distributions measured by OHZORA at the same altitudes, particularly in the South Atlantic Anomaly (SAA) region (Fung *et al.*, 1996). Quantitative discrepancies are seen, however, in both the outer and inner belt regions. At L > 5, the model fluxes are almost a factor of 10 higher than the observations within the longitudinal range of the SAA. Even lower model fluxes were obtained in other longitudes. These discrepancies may be artifacts of the use of a tilted, but symmetric dipole magnetic field in the model calculations.

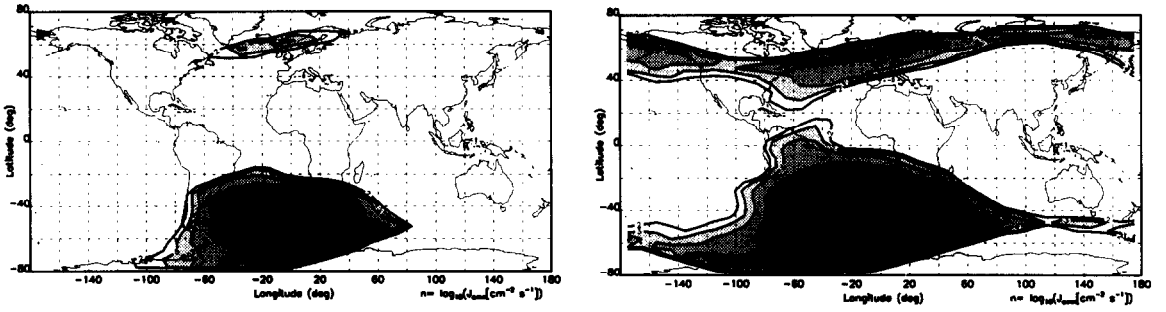

Figure 3. Model calculations of global distributions of omnidirectional fluxes of trapped electrons (> 0.2 MeV) at 400 km (left) and 800 km (right). The five contour levels vary logarithmically from 10^2 to 10^6 $cm^{-2}s^{-1}$.

At L < 2, the SAA is observed to have a greater latitudinal, but lesser longitudinal, extent than the model results. In this case, we note that the apparent latitudinal extension of the inner radiation belt may have resulted from contamination of the OHZORA electron measurements by high energy protons. The horn in the distribution at 800 km in the northern part of South America appears also in the observations (Fung *et al.*, 1996).

Figure 4 compares the Salammbo and AE8MIN models to the OHZORA measurements. Since the AE8 model predicts vanishingly small trapped electron fluxes at altitudes below the magnetic cutoff, *i.e.* $B > B_c$, with $B_c/B_0 = bc2 = 0.6572\ L^{3.452}$ for $1.2 < L < 2.4$ (Vette, 1991), this condition was taken as a virtual trajectory in the L-B/B_0 plane (where B is the local magnetic field strength and B_0 is its equatorial value along the same field line). Therefore we compare the model predictions and observations along three virtual trajectories located above (i.e., at higher altitude with $B/B_0 = 0.9$ bc2; top panel), at (B/B_0 = bc2 ; middle panel), and below (B/B_0 = bc2 ; bottom panel) the AE8 magnetic cutoff.

In the outer radiation belt region (3 < L < 5), the low-altitude L-shell profiles computed from both the Salammbo and AE8 models are quite similar to their equatorial counterparts (Figure 2). Despite their relative discrepancies, both models are consistent with the OHZORA observations. The slightly higher model fluxes than the measurements may be attributed to inaccurate radial diffusion coefficients at low pitch angles or latitudinal wave distributions (Figure 1) in that region. The overall agreement between the Salammbo model and the OHZORA measurements for this altitude (350 - 850 km) and energy ranges (E > 0.2 MeV) is quite remarkable.

Quite different performance of the models are seen in the low L-shell range (L < 3), shown in Figure 4. For very low altitude trajectories (bottom panel), the AE8 model predicts vanishingly small population of trapped electrons, but both the Salammbo model and observations are at least two orders of magnitude higher in fluxes. Above the AE8 cutoff (top panel), the AE8 model is consistent with the OHZORA observations except for a displacement of the slot region ($\Delta L \sim 0.5$); but the Salammbo model predicts the trapped electron fluxes to be near the observed upper limits. Near the upper L-shell boundary the Salammbo model seems to perform most poorly below the cutoff between L = 5 and 7. This can be due to deficiencies in AE8 which sets the boundary conditions of the Salammbo code at L = 7 and to the uncertainties in the plasmaspheric hiss distribution (Figure 1).

Figure 4 clearly indicates that the AE8-MIN model is deficient at low L shells (L < 3) and at low altitudes. At L = 2 below the cutoff, a minimum of 5 orders of magnitude difference in fluxes is found between the measurements and the AE8MIN model. The Salammbo model is clearly much better, including the prediction of the slot location.

SUMMARY AND CONCLUSIONS

Good agreement in low altitude L-shell profiles of trapped electrons has been found between the diffusive Salammbo model and *in situ* observations by OHZORA at L < 5 . The classical diffusive model also performs better than AE8 model in terms of predicting the radiation belt structure at low altitudes for L < 3 and E > 0.2 MeV. At L > 5, the discrepancies between the diffusive model and measurements are attributable to (1) inaccuracies of AE8 at low altitude and L near 7, (2) inaccuracies in D_{LL} at low pitch angles, and (3) uncertainties in plasmaspheric hiss distribution. Possible improvements of the diffusive model calculations may also include increasing the resolutions in M, J, L, and time so that dynamics effects of the outer radiation belt and geomagnetic activity-dependent transport can be included for the construction of a new generation of trapped radiation models (Fung, 1996).

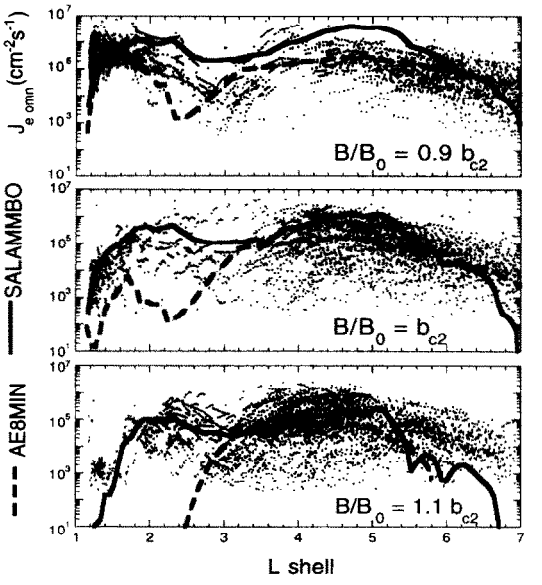

Figure 4. L-shell profiles of trapped electrons (0.19-3.2 MeV) observed by OHZORA at 350-850 km during quiet times ($|D_{st}|$<30nT) in 1984-87. The corresponding profiles along three different low altitude tracjectories (magnetic cutoffs) as computed from the Salammbo and NASA AE-8MIN models are shown in solid and dashed lines, respectively.

ACKNOWLEDGMENTS

We thank Drs. T. Kohno (IPCR, Saitama, Japan) and K. Nagata (Tamagawa University, Tokyo, Japan) for providing the OHZORA data to the National Space Science Data Center (NSSDC).

REFERENCES

Baker, D. N., J. B. Blake, L. B. Callis, J. R. Cummings, D. Hovestadt, S. Kanekal, B. Klecker, R. A. Mewaldt, and R. D. Zwickl, Relativistic electron acceleration and decay time scales in the inner and outer radiation belts: SAMPEX, *Geophys. Res. Lett.*, **21**, 409-412, 1994.

Beutier, T., and D. Boscher, A three-dimensional analysis of the electron radiation belt by the Salammbo code, *J. Geophys. Res.*, **100**, 14853-14861, 1995.

Fung, S. F., Recent development in the NASA trapped radiation models, *Proceedings of Radiation Belt Workshop: Models and Standards*, Brussels, Belgium, in press, 1996.

Fung, S. F., L. C. Tan, D. Bilitza, D. Boscher, and J. F. Cooper, An investigation of the spatial variations of the energetic trapped electrons at low altitudes, *Adv. Space Res.*, to be published, 1996.

Kohno, T., K. Munakata, K. Nakada, H. Murakami, A. Nakamoto, N. Hasebe, J. Kikuchi, and T. Doke, Intensity maps of MeV electrons and protons below the radiation belt, Planet. Space Sci., **38**, 483, 1990.

Lyons, L. R., and R. M. Thorne, Equilibrium structure of radiation belt electrons, J. Geophys. Res., **78**, 2142, 1973.

Lyons, L. R., R. M. Thorne, and C. F. Kennel, Pitch-angle diffusion of radiation belt electrons within the plasmasphere, J. Geophys. Res., **77**, 3455, 1972.

Nagata, K., T. Kohno, H. Murakami, A. Nakamoto, N. Hasebe, T. Takenaka, J. Kikuchi, and T. Doke, OHZORA high energy particle observations, J. Geomag. Geoelectr., **37**, 329, 1985.

Roederer, J. G, *Dynamics of Geomagnetically Trapped Radiation*, Springer-Verlag, New York, 1970

Schulz, M, *Geomagnetism*, **4**, Academic Press, New York, 87-293, 1991

Schulz, M. and L. J. Lanzerotti, *Particle Diffusion in the Radiation Belts*, Springer-Verlag, New York, 1974.

Spjeldvik, W. N. and P. L. Rothwell, The Radiation Belts, in *Handbook of Geophysics and the Space Environment*, edited by A. S. Jura, Air Force Geophysics Laboratory, pp. 5-1 – 5-55, 1985.

Thorne, R. M., E. J. Smith, R. K. Burton, and R. E. Holzer, Plasmaspheric hiss, *J. Geophys. Res.*, **78**, 1581, 1973.

Vette, J. I., *The AE-8 Trapped Electron Model Environment*, NSSDC/WDC-A-R&S **91-24**, NASA Goddard Space Flight Center, Greenbelt, Maryland, November, 1991.